Isı Bilimi ve Tekniği Dergisi, 42, 1, 37-48, 2022
J. of Thermal Science and Technology
©2022 TIBTD Printed in Turkey
ISSN 1300-3615
https://doi.org/10.47480/isibted.1107429

NUMERICAL ANALYSIS OF MICROWAVE CANCER THERAPY USING SINGLE AND DOUBLE SLOT ANTENNAS FOR BREAST AND LIVER TISSUES

Aykut EREN*, Zeynep AYTAÇ, Oğuz TURGUT*** and Burak TIĞLI******
*Gazi Üniversitesi Mühendislik Fakültesi Makina Mühendisliği Bölümü
06570 Maltepe, Ankara
*aykuteren5@gmail.com, ORCID: 0000-0003-2356-9331
**zeynepaytac@gazi.edu.tr, ORCID: 0000-0003-0717-5287
***oturgut@gazi.edu.tr, ORCID: 0000-0001-5480-1039
****buraktigli@gmail.com, ORCID: 0000-0003-1027-9247

(Geliş Tarihi: 22.09.2021, Kabul Tarihi: 21.02.2022)

Abstract: Microwave cancer therapy is an effective method used to destroy cancer cells which eliminates the need for surgical intervention in diseases such as breast and liver cancer. The present study aims to present a methodology for the destruction of killing the malignant cells in a wider periphery by means of burning in a shorter time meanwhile causing minimal damage to the healthy tissues. The study is carried out for a frequency value of 2.45 GHz and for a power value of 10 W using finite element methods. A comparison between coaxial single-slot antenna and double-slot antenna is conducted for liver and breast tissues. Investigated parameters are the slot number, the type of the tissue and the duration of microwave cancer therapy. The specific absorption rate and temperature distribution are the examined parameters. The results of the study show that both peak specific absorption rate and peak temperature value are obtained for microwave coaxial single slot antenna within the liver tissue, and it is observed that the temperature distribution depends on time. Maximum temperature value is attained as 93.9°C and 82.8°C for single and double slot antennas for liver tissue whereas the so-called values are 93.0°C and 69.8°C for breast tissue. New correlations are given for the treatment of liver and breast tissues using coaxial single slot antenna. It is anticipated that the present study makes a contribution in the field of medicine.
Keywords: Microwave ablation technique, Microwave coaxial antenna (MCA), Specific absorption rate (SAR), Effective wavelength, Finite element method

MEME VE KARACİĞER DOKULARINDA TEK VE ÇİFT YUVALI ANTEN KULLANILARAK YAPILAN MİKRODALGA KANSER TEDAVİSİNİN NÜMERİK ANALİZİ

Özet: Mikrodalga tedavisi, meme ve karaciğer kanseri gibi hastalıklarda, kanserli hücreleri yok etmek için cerrahi müdahale ihtiyacını ortadan kaldırabilen etkili bir yöntemdir. Mevcut çalışma, malign hücrelerin daha geniş bir çevrede, daha kısa sürede yakılırken çevre dokulara en az hasara sebep olmayı amaçlayan bir metodoloji sunmaı hedeflemektedir. Bu çalışma, 2.45 GHz frekans ve 10 W güç değeri kullanılarak sonlu eleman metoduyla gerçekleştirilmiştir. Meme ve karaciğer dokularında, eş eksenli tek yuvalı ve çift yuvalı antenler için bir kıyaslama sunulmuştur. Araştırılan parametreler yuva sayısı, doku tipi ve mikrodalga kanser tedavisinin süresi iken sonuçta incelenen parametreler özgül soğrulma oranı ve sıcaklık dağılımıdır. Çalışmanın sonucunda, hem en yüksek özgül soğrulma oranı hem de en yüksek sıcaklık değeri, karaciğerde tek yuvalı antenle elde edilmiştir ve elde edilen sıcaklık dağılımının zamana bağlı olduğu görülmüştür. Karaciğerde elde edilen en yüksek sıcaklık değeri, tek yuvalı antende 93.9°C ve çift yuvalı antende 82.8 °C olmuştur. Aynı değerler meme dokusunda, tek yuvalı antende 93.0 °C ve çift yuvalı antende 69.8 °C olarak kaydedilmiştir. Tek yuvalı anten için, karaciğer ve meme dokularının tedavisinde kullanılmak üzere yeni korelasyonlar sunulmuştur. Yapılan çalışmanın, tıp alanında katkı sağlaması beklenmektedir.
Anahtar Kelimeler: Mikrodalga ablasyon tekniği, Mikrodalga eş eksenli anten, Özgül soğurma değeri, Efektif dalga boyu, Sonlu elemanlar metodu

NOMENCLATURE

c	Speed of light in free space [$m \cdot s^{-1}$]	E	Electric field [$V \cdot m^{-1}$]
C	Heat capacity of tissue [$J \cdot kg^{-1} \cdot °C$]	f	Microwave frequency [GHz]
C_b	Heat capacity of blood [$J \cdot kg^{-1} \cdot °C$]	H	Magnetic field [A/m]
		k	Propagation constant [m^{-1}]
		L	Arc length [m]

n	Normal vector
P	Input microwave power [W]
$\dot{Q}_{ext}$	External heat source [W·m^{-3}]
$\dot{Q}_{met}$	Metabolic heat source [W·m^{-3}]
r, z	Components of cylindrical coordinates [m]
r_i	Inner radius of the coaxial cable [m]
r_o	Outer radius of the coaxial cable [m]
t	Time [s]
T	Temperature [°C]
T_b	Blood Temperature [°C]
Z	Wave impedance in the dielectric of the coaxial cable [Ω]
ε_o	Permittivity of free space [F/m]
ε_r	Relative permittivity [-]
λ	Wavelength [m]
λ_{eff}	Effective wavelength [m]
μ_o	Permeability of free space [H/m]
ρ	Density of the tissue [kg/m^3]
ρ_b	Blood density [kg·m^{-3}]
σ	Electrical conductivity of tissue [S·m^{-1}]
σ_{el}	Electrical conductivity [S·m^{-1}]
ω	Angular frequency [rad/s]
ω_b	Blood perfusion rate [s^{-1}]
MCA	Microwave coaxial antenna
PTFE	Polytetrafluoroethylene
SAR	Specific absorption rate

INTRODUCTION

Throughout the world, the most frequently encountered and diagnosed types of cancer are female breast (11.7%), lung (11.4%), colorectal (10%), prostate (7.3%), and stomach (5.6%) cancer while the terminal types are mostly lung (18.0%), colorectal (9.4%), liver (8.3%), stomach (7.7%) and female breast (6.9%) cancers in 2020 (Sung *et al.,* 2021). The traditional treatment methods for liver and breast cancer are surgical operation, heating/hyperthermia (radiofrequency ablation, microwave ablation, laser), freezing (cryosurgery), chemotherapy or radiation therapy (radiotherapy) depending on the current situation of the patient. Hyperthermia method can be implemented to a local point, to a regional area or to the entire body (Rubio *et al.*, 2011). The microwave cancer treatment is a type of the hyperthermia method which is applied locally.

Microwave cancer therapy, also known as thermal therapy/thermotherapy, is one of the methods used in cancer treatment by exposing the maligned tissue to high temperature. Radiofrequency waves which are transmitted from the tip of microwave antenna causes heating as a result of the increased kinetic energy of polar water molecules (Kaur and Mann, 2014).

Damaging the proteins and structures within the cancer cell cause the tumors to shrink, and finally these cells end up dead. The advantages of the microwave cancer therapy method are heating the zone in a shorter time as well as reaching wider lesions with blood perfusion.

Three types of antennas (monopole, dipole, and slot) are commonly encountered in using microwave cancer therapy due to their low cost, simple design and small dimensions. Literature investigation has shown that many researchers have studied the cancer treatment using microwave ablation method with slot antenna.

Rubio et al. (Rubio *et al.,* 2011) modeled double slot antenna employing two different numerical methods, the finite element method and a finite-difference time-domain. Kaur and Mann (Kaur and Mann, 2014) conducted a study to compare the results of coaxial single and double slot antennas at a frequency of 2.45 GHz and at a power of 10 W for liver tissue. Rossetto and Staufer (Rossetto and Staufer, 1999) examined the effect of bolus –tissue load on SAR distribution at a frequency of 915 MHz using finite difference time domain method. Hamada et al. (Hamada *et al.,* 2000) studied the electric field and the SAR distribution inside the human body (muscle) using finite difference time domain method by using four different antennas. Kim and Rahmat-Samii (Kim and Rahmat-Samii, 2004) numerically studied a cancer cell located in brain using single slot dipole antenna. Keane et al. (Keane *et al.,* 2011) examined the thermal profiles for cardiac tissue using monopole antenna at a frequency of 2.45 GHz. Keangin et al. (Keangin *et al.,* 2011) investigated the effects of a single and double slot coaxial antennas for liver tissue using finite element method. Jiao et al. (Jiao *et al.,* 2012) calculated SAR value and temperature distribution for ex vivo pork liver by means of finite element analysis using coaxial slot antenna. Acikgoz and Turer (Acikgoz and Turer, 2014) conducted a study to investigate the effect of T-ring shape mounted on the outer conductor of the structure using microwave coaxial slot antenna for the treatment of liver cancer; SAR and backward heating effects were investigated. Zafar et al. (Zafar *et al.,* 2014) used the single and double slot antennas to compare SAR distribution using finite element method for liver tissue. Rubio et al. (Rubio *et al.,* 2015) numerically investigated the microwave ablation in breast cancer using a coaxial slot antenna. Razib et al. (Razib *et al.,* 2016) focused on antenna's slot position within the breast tissue. SAR and temperature distribution were studied, and it was stated that the slot position of the antenna is substantial for the treatment of cancer tissue. Keangin and Rattanadecho (Keangin and Rattanadecho, 2013) numerically investigated the heat transport for local thermal non-equilibrium in porous liver during microwave ablation using finite element method. Keangin and Rattanadecho (Keangin and Rattanadecho, 2018) conducted a study presenting a numerical simulation of microwave ablation using single slot antenna on the tumor layer and the normal tissue which made up the layers of porous liver tissue. Uzman et al. (Uzman *et al.,* 2020) investigated the problem of backward heating in microwave ablation, and they proposed an electromagnetic solution based on the utilization of high impedance graphene material. They analyzed the effects of graphene layer to the heat dissipation in the maligned tissue and the duration of the treatment.

Selmi et al. (Selmi *et al.,* 2020) presented a study about the utilization of the finite element method for liver tissue. They analyzed the electro-thermal effects, temperature distribution profile, SAR, and the fraction of the necrotic tissue within the maligned cells. Tehrani et al. (Tehrani *et al.,* 2020) searched the effects of the shape and size of the tumor on microwave ablation. The coupled bio-heat and electromagnetic equations were solved to obtain the temperature gradient by using a three-dimensional finite element method. In addition, the distance between two slots in the coaxial double slot antenna was modified targeting the best treatment. They concluded that the treatment of larger tumors is harder than the smaller ones.

Literature review revealed that the effect of body type for the cancer treatment using microwave ablation method with slot antenna has not been studied at the mentioned frequency. Therefore, this study concerns the treatment of cancer located in liver and breast tissues by using antenna at the frequency of 2.45 GHz and power of 10 W (Keangin *et al.,* 2011). The investigated parameters are the number of slots, type of the tissue and the duration of the process. Temperature distribution and SAR are examined. The novelty of this study is the investigation of the effect of body type for the cancer treatment using microwave ablation method with slot antenna. Giving the new correlations for the treatment of liver and breast tissues is another innovative aspect of this study.

MATERIAL PROPERTIES AND MODELS

Figure 1 shows the simulation of antennas embedded in the tissue. The antenna is encased in the catheter. Frequency and microwave power are transmitted by antenna to the tissue. Radiation is dispersed to the cell by the radiation port.

The geometries of single and double slot microwave antennas used in this study are shown in Figure 2 for liver and breast tissues. In Figure 2, z and r represents the insertion depth and arc length, respectively. The utilized antenna has a radius of 0.895 mm, i.e., it is excessively thin, which makes it possible to embed it inside the tissue easily. The material of the inner conductor is silver plated copper, and it has a radius of 0.135 mm. The outer conductor is made from copper, and the radius is 0.335 mm. In addition, the slot has a width of 1 mm. The antenna is enclosed in a catheter as mentioned before.

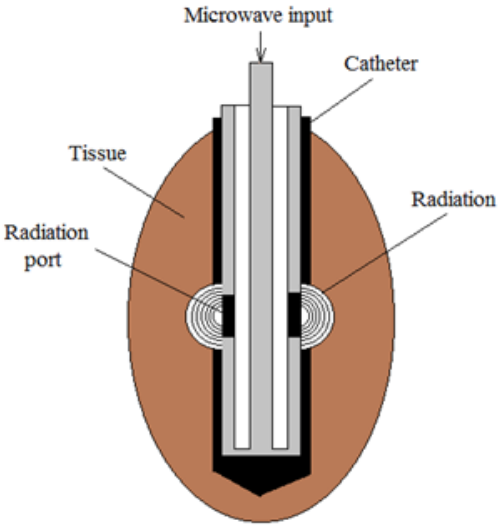

Figure 1. Antenna embedded in a tissue

The catheter is made from polytetrafluoroethylene (PTFE). PTFE has a high dielectric strength, and it is a heat resistant material (-200°C to 260°C). Another advantage of PTFE is that it does not react with any chemicals.

The electric field becomes stronger as the distance to the slot decreases, which causes the maximum temperature to be obtained near the slot. The antenna is based on a 50Ω UT-085B-SS, and it is stainless steel. Microwave frequency operating at 2.45 GHz is applied to heat the tissue (Rubio *et al.,* 2011), (Kaur and Mann, 2014), (Keangin *et al.,* 2011). Microwave ablation therapy transmits energy to the body in shorter wavelengths compared to the other methods. The spacing of slots in the tissue based on the effective wavelength at the frequency of 2.45 GHz is determined by (Rubio *et al.,* 2011), (Keangin *et al.,* 2011).

$$\lambda_{eff} = c/f\sqrt{\varepsilon_r} \quad (1)$$

where c is the speed of light in free space, and ε_r is the relative permeability of tissue at the operating frequency. f represents the operating frequency of the microwave generator, and it has a value of 2.45 GHz.

The relative permeability of liver and breast tissues are different from each other. In other words, the slot spacing length of the mentioned tissues are not equal. For double slot microwave coaxial antenna, the slot spacing length of the liver tissue is 4.5 mm, whereas it is 13 mm for the breast tissue.

The properties of liver and breast tissues used in the present study are given in Table 1 (Rubio *et al.,* 2011), (Kaur and Mann, 2014), (Razib *et al.,* 2016). The properties of the dielectric material and catheter are represented in Table 2 (Kaur and Mann, 2014), (Razib *et al.,* 2016).

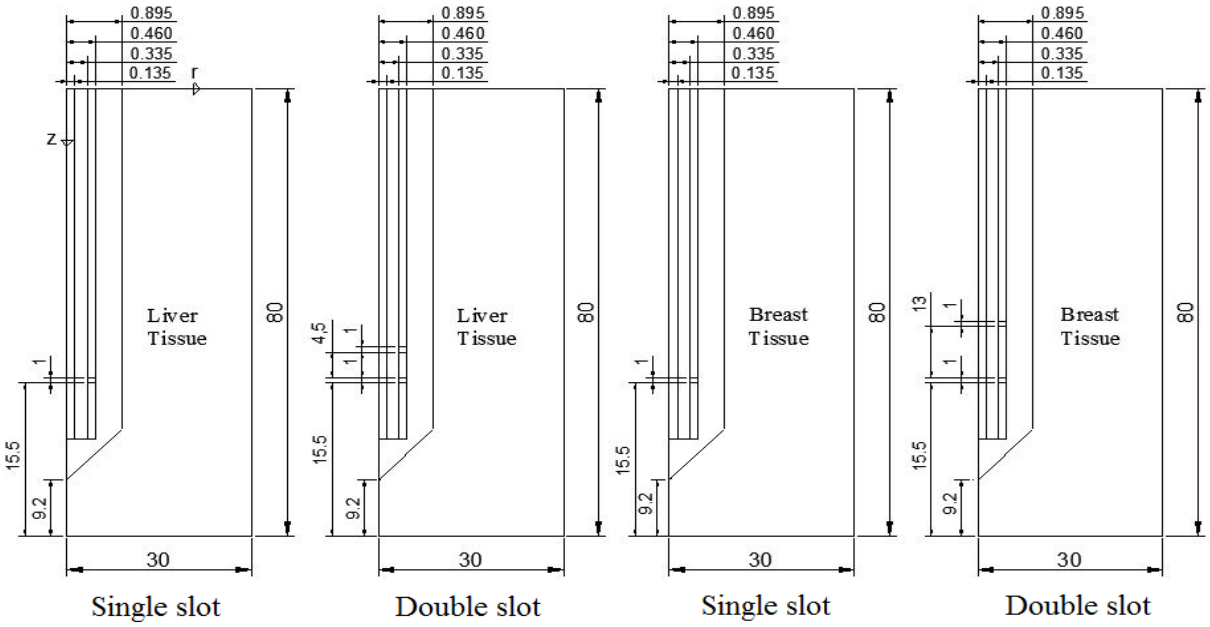

Figure 2. Single and double slot microwave antenna geometries for breast and liver tissues (Dimensions are in mm)

Table 1. The properties of liver and breast tissues

Property Name	Liver	Breast
Heat capacity	4187 (J·kg^{-1}·K)	2960 (J·kg^{-1}·K)
Density	1038 (kg·m^{-3})	1058 (kg·m^{-3})
Relative permittivity	45.2	5.14
Electric conductivity	2.12 (S·m^{-1})	0.137 (S·m^{-1})
Thermal conductivity	0.5 (W·m^{-1}·K^{-1})	0.42 (W·m^{-1}·K^{-1})
Blood temperature	310K	310K
Blood perfusion rate	3.6×10^{-3} s^{-1}	3.6×10^{-3} s^{-1}

Table 2. The properties of dielectric material and catheter

Property Name	Value
Relative permittivity of dielectric	2.03
Relative permittivity of catheter	2.6
Relative permeability	1
Thermal conductivity of PTFE	0.25 (W·m^{-1}·K^{-1})
Density of PTFE	2200 (J·kg^{-1}·K)
Heat capacity of PTFE	1300 (J·kg^{-1}·K)
Microwave power input	10 W
Microwave frequency	2.45 GHZ

Thermal Analysis

The temperature distribution inside the tissue is calculated by Pennes' bioheat equation given by Eq. (2).

$$\rho C \frac{\partial T}{\partial t} = k\nabla^2 T - \rho_b C_b W_b (T - T_b) + \dot{Q}_{met} + \dot{Q}_{ext} \quad (2)$$

where ρ, C, T and k represent the density, heat capacity, temperature, and thermal conductivity of the tissue, respectively, whereas ρ_b, C_b, W_b and T_b indicate the density, specific heat capacity, perfusion rate, and temperature of the blood, respectively. The first term on the right-hand side of Eq. (2) represents the heat conduction inside the tissue, and second term describes the heat caused by convection. $\dot{Q}_{met}$ is the metabolic heat generation within the tissue. $\dot{Q}_{ext}$ is the external heat source (electromagnetic) term which can be calculated by equation

$$\dot{Q}_{ext} = \frac{\sigma E^2}{2} \quad (3)$$

where σ represents the tissue conductivity [S/m], and E is the electric field within the tissue [V/m].

Boundary conditions

Thermal insulation boundary condition is applied to the external boundary of the computational domain, i.e., n.(k∇T)=0.
Initial temperature is considered to be T_o=T_b=37°C.

Electromagnetic Analysis

The microwave treatment is a multi-physics problem, and it involves the coupling of the temperature and electromagnetic fields. Electric ($\vec{E}$) and magnetic ($\vec{H}$) fields are expressed as Keangin *et al.*, 2011), (Keangin and Rattanadecho, 2013), (Keangin and Rattanadecho, 2018), (Bertram *et al.*, 2006), (Liu *et al.*, 2013).

$$\vec{E} = \vec{e}_r \frac{A}{r} e^{\sqrt{-1}(\omega t - kz)} \quad (4a)$$

$$\vec{H} = \vec{e}_\varphi \frac{A}{rZ} e^{\sqrt{-1}(\omega t - kz)} \quad (4b)$$

with $Z=\sqrt{\mu_o/\varepsilon_r\varepsilon_o}$ is the wave impedance in the dielectric of the coaxial cable [Ω], $\mu_o=4\pi\times10^{-7}$ is the permeability of free space [H/m], ε_r is is the relative permittivity of the dielectric, $\varepsilon_o=8.854\times10^{-12}$ is the permittivity of free space [F/m], P is the input power [W], r_i and r_o are the inner and outer radii of the coaxial cable [m], $\omega=2\pi f$ is the angular frequency [rad/s], f is the frequency [Hz], $k=2\pi/\lambda$ is the propagation constant [m^{-1}], λ is the wavelength [m], and t is the time [s].

At the antenna symmetry axis $\vec{E}_r = 0$ and $\frac{\partial \vec{E}_z}{\partial r} = 0$ boundary conditions are applied. In addition, $\vec{n}\times\sqrt{\varepsilon}\vec{E} - \sqrt{\mu}H_\varphi = -2\sqrt{\mu}\vec{H}_{\varphi_o}$ boundary condition is applied to the outer boundaries of the computational domain. The local specific absorption rate (SAR) is calculated using the relation

$$SAR=\frac{\sigma}{\rho}\left|\vec{E}\right|^2 \quad (5)$$

where σ indicates the tissue conductivity [S/m], ρ is the density of the tissue [kg/m^3], and E represents electric field within the tissue [V/m]. It can be seen from Eq. (5) that the SAR value is dependent on the square of the electric field generated around the antenna. The calculated SAR value is equivalent to the heating source created by the electric field. Although the SAR value does not directly determine the final temperature distribution of the tissue, it causes the temperature to increase (Rubio *et al.*, 2011). This result stems from the application of power for a specific duration.

Computational Method

COMSOL Multiphysics software based on finite element method is used to simulate the problem. A non-uniform mesh distribution is employed, and the typical mesh distribution is shown in Fig. 3 for coaxial single slot antenna. The compactness of the grid structure is increased as getting closer to the antenna in order to enhance the resolution and accuracy of the solution. Mesh independence study is conducted by improving the quality of the mesh structure until the variation in the maximum temperature of the tissue becomes negligible. The computations are performed using a range of element numbers varying from 3114 to 30719 to investigate the effect of the element size on the solution and to ensure that the attained results are independent of the mesh structure. The obtained maximum temperature values for five different grid sizes are given in Table 3. It is observed that the mesh structure having 30719 elements gives the optimum solution, and a similar procedure is followed for double slot antenna.

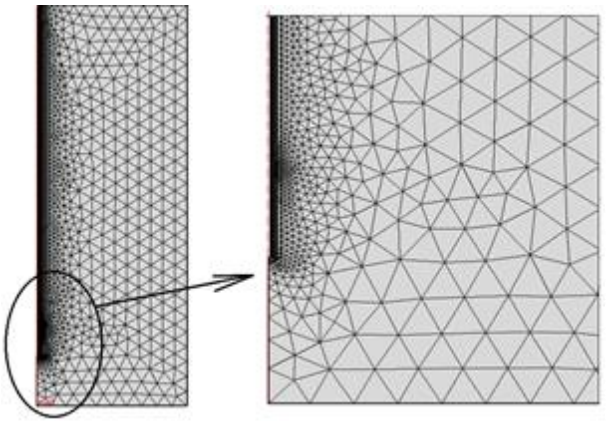

Figure 3. Typical mesh distribution

Table 3. Maximum temperature values for different element numbers

Mesh quality	Normal	Finer	Extra Fine	Extremely Fine	Used Mesh
Element number	3114	3903	5627	13520	30719
Maximum temperature (°C)	93	93.1	93.1	93.1	93.09

RESULTS AND DISCUSSION

Verification of the Numerical Study

The numerical study of Keangin et al. (2018) is repeated here to ensure the accuracy of the present numerical study. Verification was carried out for single and double slot coaxial antennas for liver tissue at a frequency of 2.45 GHz and at a power of 10 W. The comparison of the obtained temperature distributions of the current study and of Keangin et. al.'s (2018) study is represented in Figure 4.

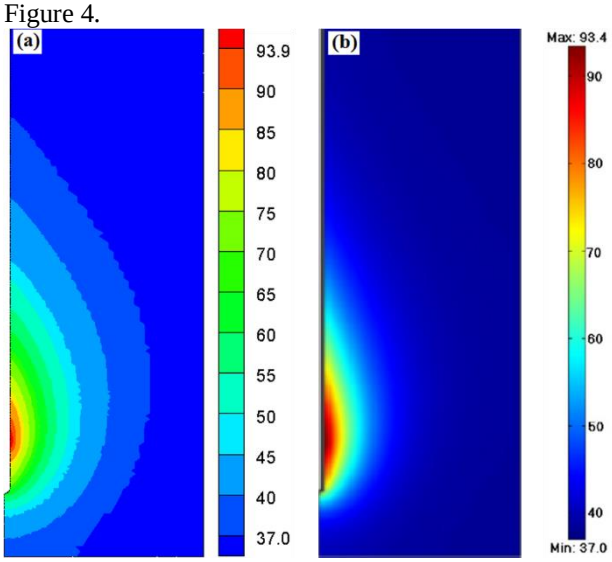

Figure 4. Temperature distribution after 300 second; (a) present and (b) literature study (Keangin *et al.*, 2011)

It is found out that the maximum temperature obtained for single slot after 300 seconds is 93.9°C for the current study, and it is 93.4°C for Keangin et al.'s study [8]. In addition, the attained peak SAR value for double slot is

2.49 kW/kg and 2.37 kW/kg for this study and Keangin et al.'s (Keangin *et al.*, 2011) study, respectively. It can be concluded that the results of present study are in good agreement with that of Keangin et al. (Keangin *et al.*, 2011).

SAR Distribution

Figure 5 represents the SAR distribution throughout the insertion depth (z-axis) at 0.895 mm (approximately r=1 mm) for single slot and double slot microwave coaxial antenna (MCA) in liver and breast tissues. A microwave power 10 W is applied to the tissues for 300 seconds at a frequency of 2.45 GHz.

Considering the liver tissue, when single and double slot MCAs are compared, it is seen that the peak SAR value is 3058 W·kg-1 at the insertion depth of z=62.8 mm for single slot MCA. For double slot MCA, it is obtained that the peak SAR value is 2490 W·kg-1 at the insertion depth of z=59.6 mm. The SAR value decreases abruptly after the peak value, and this trend keeps continuing until the arc length is 80 mm. In addition, it is deduced that the value of SAR depends on the number of slots. It is presumed that a lower SAR value for the double slot antenna is a result of the dispersed frequency from the slots.

For the breast tissue, it is seen that the peak SAR value is 1961 W·kg-1 at the insertion depth of z=68.1 mm for the single slot. However, two peak SAR values are obtained for double slot MCA. This value is found to be 870 W·kg-1 at an insertion depth of 51.1 mm and 1304.5 W·kg-1 at that of 68.6 mm. It is seen that the maximum SAR values occur near the slots. After the peak value is passed, SAR decreases suddenly whose minimum value is obtained at an insertion depth of 80 mm, exhibiting a similar behavior to that of the liver tissue.

The distance between the double slots for the liver tissue is smaller than that of breast tissue. Thus, it is foreseeable that the effect of microwave power decreases as the distance between two slots increases.

When the SAR values of the liver and breast tissues are compared, it is seen that a higher SAR value is obtained for the liver tissue for the equal number of slots. Also, when considering the single and double slot antennas, it is observed that utilization of single slot antenna results in a higher SAR value. The cause of having a higher SAR value for liver tissue can be interpreted as having a higher electric conductivity and smaller density. This result also can be validated from Eq. (2).

Temperature Distribution

Figure 6 shows the temperature contours for single and double slot antennas in liver and breast tissues after 300 s. An input power of 10 W was employed for single and double slot antennas with a frequency of 2.45 GHz. The left-hand side of Fig. 6 represents the temperature contours of liver tissue on the top and breast tissue on the bottom whereas the right-hand side represents the results obtained from single and double slot antennas. It is observed that the temperature value decreases as the arc length increases.

For the liver tissue, it is seen that the maximum temperature for single slot antenna is 93.9ºC at the location of r=1 mm and z=62.6 mm. Also, the peak SAR value is obtained at the same coordinates, which means that the microwave input energy is the most effective at this position. For the double slot antenna, the maximum temperature is 82.8ºC at the position r=1 mm and z=58.2 mm. The peak SAR and temperature values are obtained approximately at the same position for double slot antenna. It can be deduced that the SAR value and temperature distribution are related to each other.

When considering the liver tissue, it is seen that maximum temperature is 93.0ºC at a position r=1 mm and z=65 mm for single slot antenna. For double slot antenna the maximum temperature is 69.8ºC at a position r=1 mm and z=69 mm.

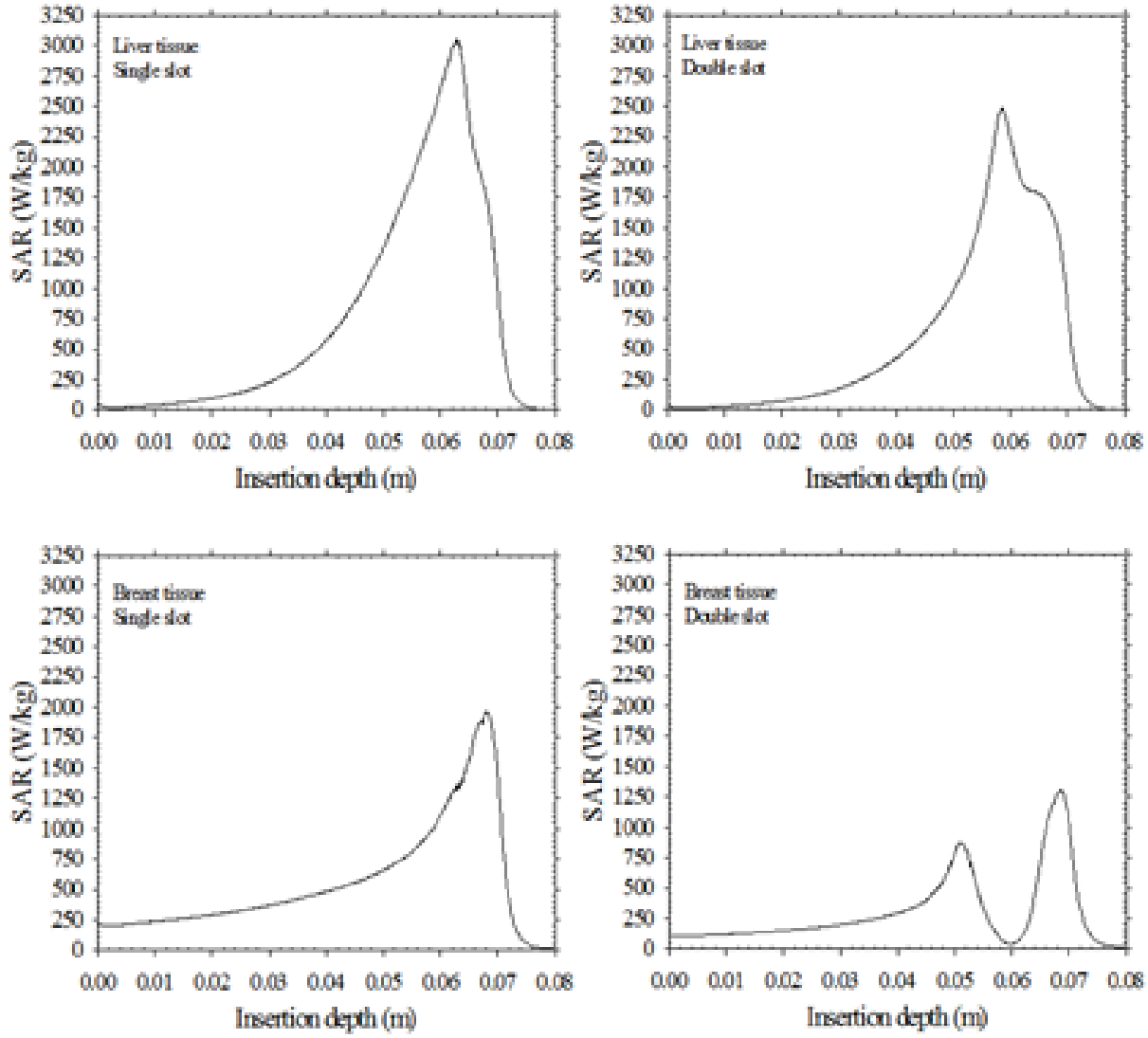

Figure 5. SAR distribution along insertion depth. From top to bottom: liver tissue and breast tissue, respectively. From left to right: single slot and double slot, respectively

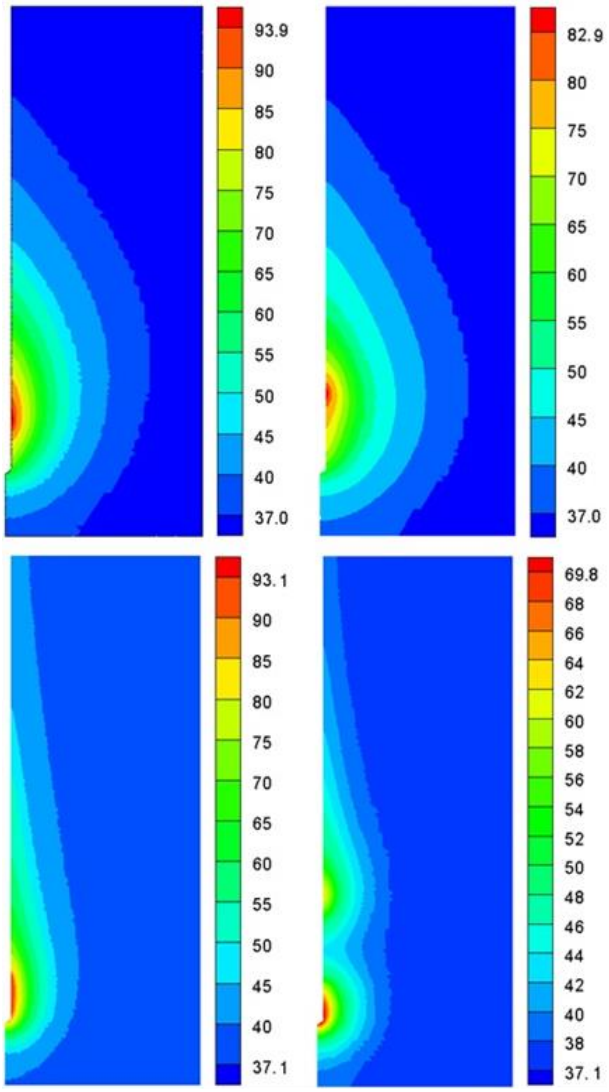

Figure 6. Temperature contour diagram. From top to bottom: liver tissue and breast tissue, respectively. From left to right: single slot and double slot, respectively

Figures 5 and 6 represent the SAR and maximum temperature values for both liver and breast tissues. It is seen that the mentioned values are found to be higher for single slot antenna when comparing to double slot. Consequently, attention will now be paid to single slot antenna. Figure 7 shows the temperature contour after 40, 100 and 300 seconds for breast and liver tissues using single slot antenna. It is seen that the heat in the tissue exhibits an ellipsoidal shape along the arc length as time passes. The maximum temperature occurs around the slot. For liver tissue, the maximum temperature is 67.1°C at the position r=1 mm and z=63 mm after 40 seconds. After 100 seconds, the maximum temperature is 80.6°C at the position r=1 mm and z=62.8 mm, and it is 93.9°C after a duration of 300 seconds at the position of r=1 mm and z=62.6 mm.

For the breast tissue, the maximum temperature is 71.4°C at the position r=1 mm and z=68.5 mm after 40 seconds. After 100 seconds, the maximum temperature is 83.0°C at the position r=1 mm and z=65 mm. This value is found to be 93.5°C at the position of r=1 mm and z=65 mm after 300 seconds. It is seen that the maximum temperature occurs approximately at the same position with increasing time concerning both tissues. In addition, it is observed that the arc length of the liver tissue is longer than that of breast tissue for the same duration.

In microwave treatments, as mentioned before, the aim is to expose the cancer tissue to heat until the temperature reaches a value of 50°C, damaging proteins and the existing structures within the cancer cell. This procedure causes the tumors to shrink, and eventually they end up dead (Rubio *et al.*, 2011), (Keangin and Rattanadecho, 2013).

Results show that the maximum arc length at a temperature of 50°C is r=3.9 mm, 6.5 mm and 9.8 mm, after 40, 100 and 300 seconds of duration in liver tissue, respectively. Regarding the breast tissue, the maximum arc length at the same temperature is r=3.3 mm, 4.8 mm and 6.6 mm, respectively, after 40, 100 and 300 seconds. In other words, it is concluded that a larger periphery of the cancer cell can be destroyed by means of increasing the duration of the procedure. It is also seen that temperature increases with increasing time.

In order to represent the temperature distribution along the arc length, temperature values are plotted as a function of arc length in Fig. 8 at an insertion depth where the temperature is maximum.

The insertion depth where temperature has a maximum value is z=62.6 mm and z=59.2 mm for single and double slot antennas in liver tissue, respectively. As for breast tissue, insertion depth where temperature has a maximum value is z=65 mm and z=69 mm for single and double slot antennas, respectively. The left-hand side of Fig. 8 represents the temperature values of liver located at the top and breast at the bottom whereas the right-hand side depicts the results obtained from single and double slots. This figure shows that the maximum temperature is obtained at r=1 mm, and also it can be deduced from the figure that the temperature decreases along the arc length. It is also seen that the temperature value in tissue for double slot begins with a lower value than that of the one having single slot. As it can be seen from Fig. 8, liver and breast tissues exhibit similar temperature distributions.

Time is plotted in Fig. 9a as a function of maximum arc length where the temperature is 50oC for liver and breast tissues. In Fig. 9a the dash-dot line is for the numerical results of the liver tissue whereas the solid line represents that of breast tissue.

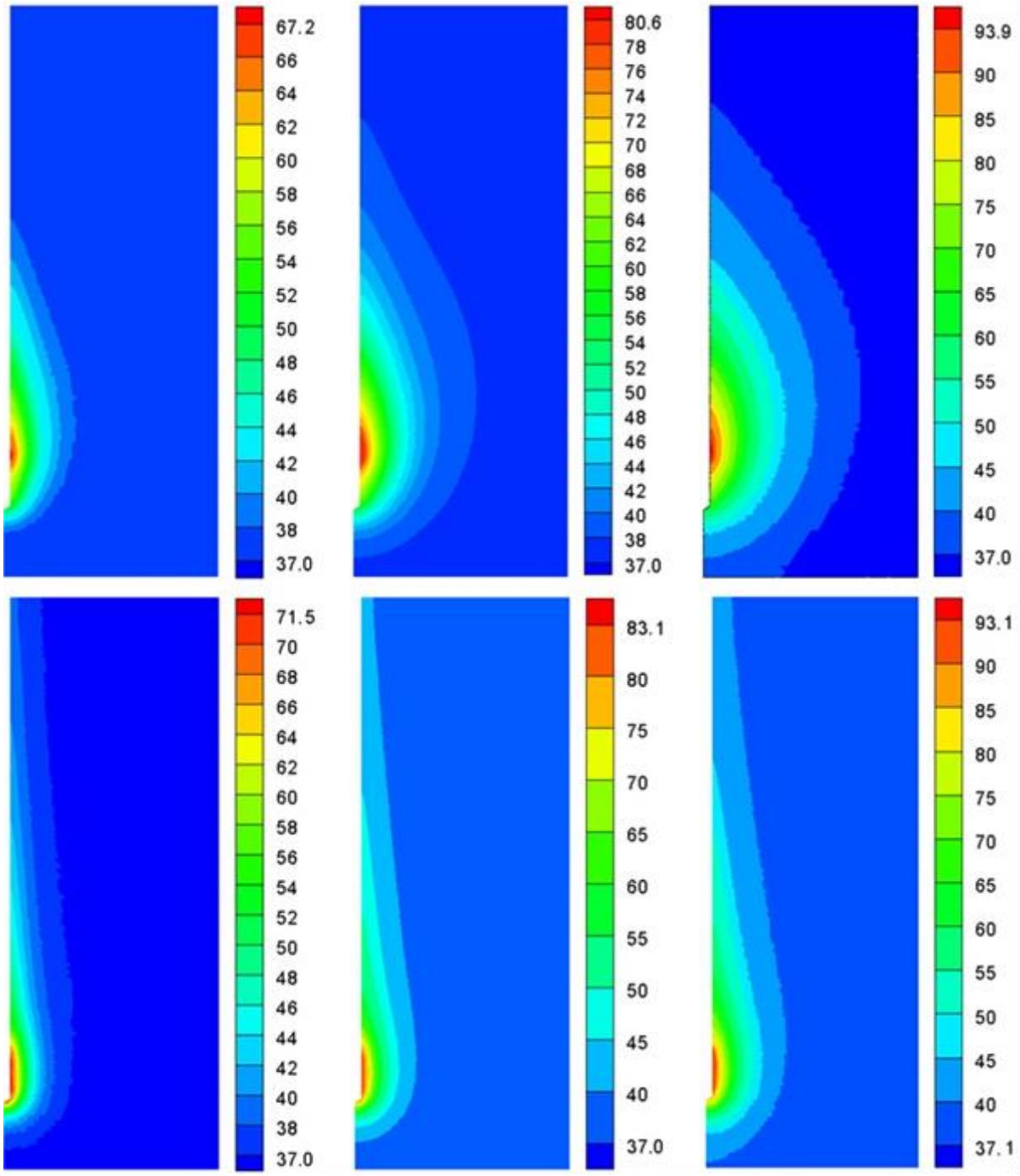

Figure 7. Temperature contour diagram. From top to bottom: liver tissue and breast tissue, respectively. From left to right: after 40s, 100s and 300s, respectively.

The results of numerical study for single slot antenna are represented by an equation in the form of

$$t(s) = aL^3 + bL^2 + cL + d \quad (6)$$

where t is the time in second, L is the maximum arc length at which temperature is 50oC (see Fig. 9b), and the unit of L is mm. In Eq. (6) a, b, c and d are the constants. Correlation equations in the form of Eq. (6) are obtained for liver and breast tissues, respectively, and are given in Eqs. (7) and (8).

$$t(s) = 0.5910L^3 - 5.476L^2 + 28.66L\text{-}22.47 \quad (7)$$
(R2=0.9989)

$$t(s) = 3.819L^3 - 34.00L^2 + 118.9L\text{-}119.1 \quad (8)$$
(R2=0.9989)

Eqs. (7) and (8) are valid for the range of $1.27 \leq L \leq 9.87$ and $1.76 \leq L \leq 6.66$, respectively. When the value of L falls out of these ranges, extrapolation can be used for these equations. The time required to destroy the cancer tissue can be calculated using Eq. (7) for breast cancer and Eq. (8) for liver cancer with knowing the arc length of the maligned tissues.

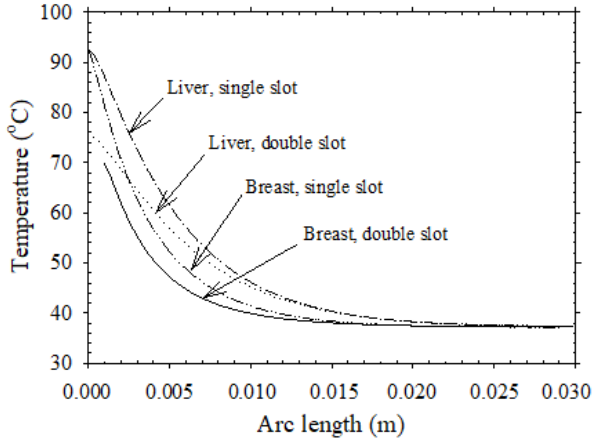

Figure 8. Temperature distribution along arc length. From top to bottom: liver tissue and breast tissue, respectively. From left to right: single slot and double slot, respectively

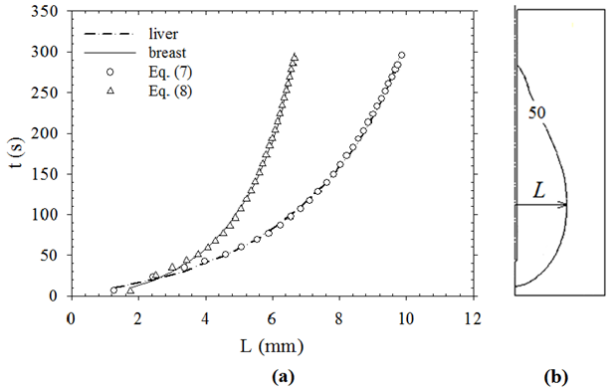

Figure 9. Time as a function of maximum arc length whose temperature is 50°C

CONCLUSION

The present study represents the modeling and analysis of single and double slot microwave coaxial antennas within breast and liver tissues by using finite element method. The study has been carried out for 2.45 GHz and 10 W. The noteworthy results are listed below;

- The temperature of the tissue increases with increasing duration.
- The characteristics of breast and liver tissues are different from each other, which results in different SAR values and temperature distributions.
- For liver tissue, maximum temperature value is 93.9oC and 82.8°C for single and double slot antennas, respectively. As for breast tissue, maximum temperature values are 93.0°C and 69.8°C for single and double slot antennas, respectively.
- The peak SAR value within the liver tissue is 3058 W·kg-1 and 2490 W·kg-1 for single and double slot antennas, respectively. For the breast tissue, the peak SAR value is 1961 W·kg-1 for single slot antenna. However; SAR value has two peak maximum values for double slot antenna in the breast tissue, and the peak SAR values are 870 W·kg-1 and 1304.5 W·kg-1.
- SAR and temperature values decrease along the arc length.
- SAR and temperature distribution strongly depend on the number and position of slot within both tissues.
- When the results of single slot and double slot antennas are compared, maximum SAR and temperature values are obtained for single slot antenna.
- When the results of liver and breast tissues are compared, maximum SAR and temperature values are obtained for liver tissue.
- Single slot antenna is more useful than double slot antenna for microwave cancer treatment. However, double slot microwave coaxial antenna has a larger ablation area.
- New correlations are given in the form of for treatment of liver and breast tissues for coaxial single slot antenna.

It is anticipated that the present study makes a contribution in the field of medicine.

ACKNOWLEDGEMENT

The authors would like to thank Nuri Eren TURKOGLU (Politecnico di Milano, Department of Electrical Engineering) for his support during the analyses.

REFERENCES

Acikgoz H. and Turer I., 2014, A Novel Microwave Coaxial Slot Antenna for Liver Tumor Ablation, *Advanced Electromagnetics*, 3, 1, 20-25.

Bertram J.M., Yang D., Converse M.C., Webster J.G. and Mahvi D.M., 2006, Antenna design for microwave hepatic ablation using an axismmetric electromagnetic model, *BioMedical Engineering OnLine*, 5:15.

Hamada L., Saito K., Yoshimura H. and Ito K., 2000, Dielectric-loaded coaxial-slot antenna for interstitial microwave hyperthermia: Longitudinal control of heating patterns, *International Journal of Hyperthermia*, 16, 3, 219-229.

Jiao T., Wang H., Zhang Y., Yu X., Xue H., Lv H., Jing X., Zhan H. and Wang J., 2012, A coaxial-slot antenna for invasive microwave hyperthermia therapy, *Journal of Biomedical Science and Engineering*, 5, 198-202.

Kaur S. and Mann P.S., 2014, Comparison of Single Slot and Double Slot Antenna for the Treatment of Hepatocellular Carcinoma, *International Journal of Research in Computer Applications and Robotics (IJRCAR)*, 2, 5, 86-91.

Keane D., Ruskin J., Norris N., Chapelon P.A. and Bérubé D., 2004, In Vitro and In Vivo Evaluation of the Thermal Patterns and Lesions of Catheter Ablation with a Microwave Monopole Antenna, *Journal of Interventional Cardiac Electrophysiology*, 10, 111-119.

Keangin P., Rattanadecho P. and Wessapan T., 2011, An analysis of heat transfer in liver tissue during microwave

ablation using single and double slot antenna, *International Communications in Heat and Mass Transfer*, 38, 757-766.

Keangin P. and Rattanadecho P., 2013, Analysis of heat transport on local thermal non-equilibrium in porous liver during microwave ablation, *International Journal of Heat and Mass Transfer*, 67, 46–60.

Keangin P. and Rattanadecho P., 2018, A numerical investigation of microwave ablation on porous liver tissue, *Advances in Mechanical Engineering*, 10, 8, 1-13.

Liu A.J., Zhou H. and Kang W., 2013, A numerical study on Microwave Coagulation Therapy, *Applied Mathematical Sciences*, 7, 104, 5151-5164.

Razib A., Hossain K.A. and Hossain S., 2016, Microwave ablation technique (MWA) for cancer treatment, *Proceedings of the 2016 International Conference on Medical Engineering, Health Informatics and Technology (MediTec)*, Bangladesh, 1-6.

Rossetto F. and Staufer P.R., 1999, Effect of complex bolus-tissue load configurations on SAR distributions from dual concentric conductor applicators, *IEEE Transactions on Biomedical Engineering*, 46, 11, 1310-1319.

Rubio M.F.J.C., Hernánde A.V., Salas L.L., Ávila-Navarro E. and Navarro E.A., 2011, Coaxial Slot Antenna Design for Microwave Hyperthermia using Finite Difference Time-Domain and Finite Element Method, *The Open Nanomedicine Journal*, 3, 2-9.

Rubio M.F.J.C., López G.D.G., Perezgasga F.V., García F.F., Hernández A.V. and Salas L.L., 2015, Computer modeling for microwave ablation in breast cancer using a coaxial slot antenna, *International Journal of Thermophysics*, 36, 2687–2704.

Selmi M., Dukhyil A.A.B. and Belmabrouk H., 2020, Numerical Analysis of Human Cancer Therapy Using Microwave Ablation, *Applied Sciences*, 10, 1, 211.

Sung H., Ferlay J., Siegel R.L., Laversanne M., Soerjomataram I., Jemal A. and Bray F., 2021, Global Cancer Statistics 2020: GLOBOCAN Estimates of Incidence and Mortality Worldwide for 36 Cancers in 185 Countries, *CA-A Cancer Journal for Clinicians*, 1-41.

Tehrani M.H.H., Soltani M., Kashkooli F.M. and Raahemifar K., 2020, Use of microwave ablation for thermal treatment of solid tumors with different shapes and sizes—A computational approach, *PLOS ONE*, 15, 6.

Uzman B., Yilmaz A., Acikgoz H. and Mittra R., 2020, Graphene-based microwave coaxial antenna for microwave ablation: thermal analysis, *International Journal of Microwave and Wireless Technologies*, 1-9.

Zafar T., Zafar J. and Zafar H., 2014, Development and microwave analysis of slot antennas for localized hyperthermia treatment of hepatocellular liver tumor, *Australasian Physical & Engineering Sciences in Medicine*, 37, 673–679.